ELSEVIER

OPTICAL Materials

Thermal lensing measurements in diode-pumped Yb-doped GdCOB, YCOB, YSO, YAG and KGW

S. Chénais [a,*], F. Druon [a], F. Balembois [a], G. Lucas-Leclin [a], Y. Fichot [a],
P. Georges [a], R. Gaumé [b], B. Viana [b], G.P. Aka [b], D. Vivien [b]

[a] *Laboratoire Charles Fabry de l'Institut d'Optique, UMR 8501 du CNRS, Centre Scientifique, Bât. 503,
91403 Orsay Cedex, France*
[b] *Laboratoire de Chimie Appliquée de l'Etat Solide, ENSCP, UMR 7574 du CNRS, 11 Rue Pierre et Marie Curie
75231 Paris Cedex 05, France*

Abstract

A Shack–Hartmann wavefront sensor was used to measure thermal lensing in diode-end-pumped Yb-doped GdCOB, YCOB, YSO, YAG, and KGW crystals, under lasing or nonlasing conditions. Measured thermal lenses are aberration-free, and their focal lengths under lasing action range from 40 to 140 mm for 5 W of absorbed power. When laser action was inhibited the thermal lens dioptric power was increased significantly in most crystals, supplying evidence that nonradiative mechanisms exist. Reduction of thermal effects in a composite YCOB crystal is also investigated, as well as the dependence of thermal lensing on the emission wavelength in YSO.
© 2002 Elsevier Science B.V. All rights reserved.

PACS: 140.3480; 140.6810

1. Introduction

Scaling the output power of diode-pumped solid-state lasers is a key issue for laser sources designers. The brightness (that is the power per unit surface and per unit solid angle) of high power laser diodes is rapidly increasing, so that end-pumping of solid-state laser materials is now the most widespread way of obtaining high efficiency together with high power. However, the high pumping intensities associated with end-pumping create thermal problems that limit the scaling to

higher powers [1]: indeed, thermal lensing and thermally induced birefringence can seriously affect the laser performance and modify the resonator stability.

Prior to the design of a high power laser source, a careful study of thermal lensing must be carried out. In most materials (above all in "new" crystals) the thermomechanical and thermo-optical coefficients are not known, so that an experimental survey is the only way to access thermal lensing data.

Performing thermal lensing measurements requires a technique that is: (1) suited to end-pumped geometries and (2) able to measure thermal distortions under lasing action.

We developed a technique based on a Shack–Hartmann wavefront analyzer (HASO 32 from

---
* Corresponding author.
  E-mail address: sebastien.chenais@iota.u-psud.fr (S. Chénais).

Imagine Optic, France), and applied it to several Yb-doped crystals, under fiber-coupled diode pumping. This technique allows to measure the thermal lens and its aberrations under lasing or nonlasing conditions. We chose a direct wavefront sensing technique instead of an interferometric method because it is simpler to implement, insensitive to vibrations, and because Shack–Hartmann wavefront sensors are now commercially available and allow a very accurate determination of wavefronts, within $\lambda/150$ rms for referenced acquisitions.

Measurements have been performed on several laser materials, all doped with ytterbium ions. The interest and properties of Yb-doped materials have been extensively discussed elsewhere [2]. Our laboratories are involved in the development of new Yb-doped crystals for directly-diode-pumped tunable lasers, like GdCOB [3,4], YCOB [5] and more recently YSO [6] which are investigated here. For the sake of comparison, thermal lensing measurements have also been done on two other more "well-known" crystals, Yb:YAG [7] and Yb:KGW [8].

All these materials were pumped on their strong zero-line absorption peak, between 968 and 979 nm.

2. Experimental setup

The setup is shown in Fig. 1: it is inspired by the work of Armstrong et al. [9], but specifically suited for end-pumped geometries.

In end-pumped lasers, the main difficulty for measuring thermal lenses is that both pump and cavity beams are small on the crystal (200 μm in diameter in our case). As a consequence, measuring the exact thermal distortion undergone by the laser beam into the cavity requires that the probe beam has the same size as the laser beam. Otherwise, some spherical aberration appears on the probe beam that is not part of the real thermal lens seen by the laser.

As the probe, we used a laser diode at 670 nm coupled in a single mode fiber (57PNL053 from Melles Griot Inc.). Since just a small power is necessary, we used the diode below threshold (i.e. as a LED, emitting 100 μW). It had thus excellent properties of spatial coherence but had a small coherence length, which is desirable to avoid coherent cross-talk (interference) between the microlenses of the Shack–Hartmann sensor [9]. The very different wavelengths of probe and laser beams makes the probe able to pass through the mirrors of the cavity, and permits the measurement of the
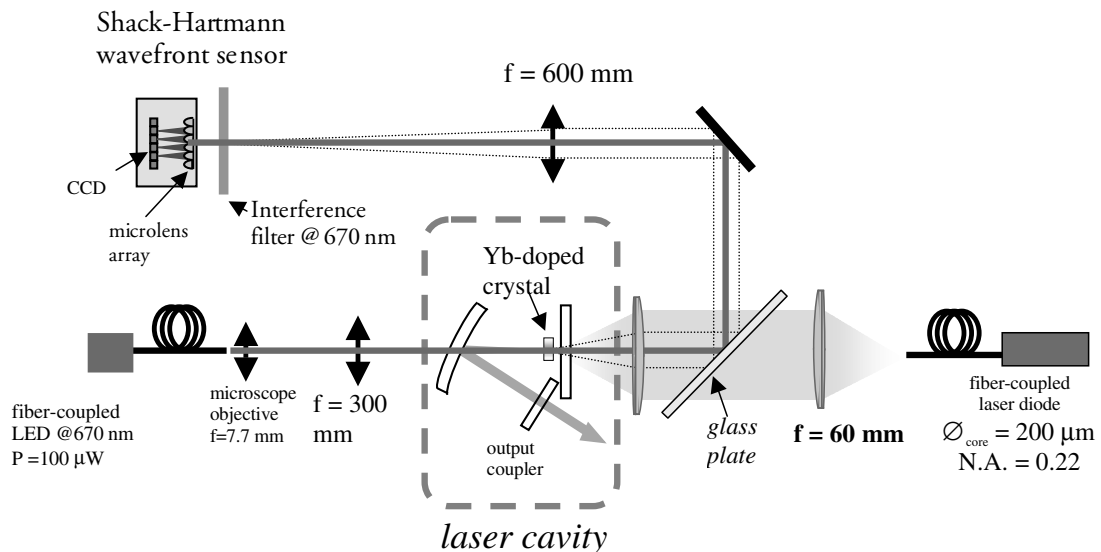

Fig. 1. Experimental setup used for thermal lensing measurements.

thermal lens under lasing action. It is a crucial point, as it will be seen in the following, since the thermal load can be very different under lasing and nonlasing conditions. In addition, the chromatic aberration of the thermal lens is negligible in common materials (the relative difference of dioptric powers between 670 nm and 1 µm is about 0.6% for YAG and GdCOB) so that no corrections have to be made in order to derive the thermal lens at 1 µm from the measurements made with the visible LED.

After collimation by a microscope objective, the probe beam was focused onto the crystal and superimposed with the pump beam. The crystal was then imaged upon the microlens array using a magnifying relay imaging system (magnification $g = 10$). The first lens was the 60 mm doublet used for focusing the pump beam into the crystal, and the second lens was a 600 mm focal length thin lens. The spacing between these two lenses was set to 660 mm, in order to guarantee that the probe wavefront is plane on the Shack–Hartmann sensor when the pump is turned off. Under these conditions the measured radius of curvature R_{mes} with the pump is related to the thermal lens focal length f_{th} by the simple relation: $R_{mes} = -g^2 f_{th}$.

An uncoated glass plate was inserted in the pump beam path to reflect the probe beam towards the sensor. A selective interference filter at 670 nm was added in front of the sensor to eliminate any unwanted signal at the pump or laser wavelengths.

A ''reference wavefront'' is recorded when the pump diode is turned off, which includes all static aberrations of the optical elements and of the cold crystal itself. It is then subtracted to the measured wavefront when the pump is on. Thus, only phase distortions originating in thermal effects are recorded. The phase front was then reconstructed by projection over the set of the orthogonal Zernike polynomials [10].

A validation of our measuring system was made with different lenses of known focal lengths: good correlation between the measured values by this method and by a classical focometry method was obtained within an accuracy of less than 5% for focal lengths ranging from 1.5 to 100 mm.

The pump source was a high power fiber-coupled diode array (HLU15F200-980 from LIMO GmbH) emitting between 12 and 14 W, at a wavelength ranging from 968 to 979 nm, set to be as closed as possible of the absorption peak of the studied material. The fiber had a core diameter of 200 µm and a numerical aperture of 0.22, and its exit face was relay-imaged onto the crystal with two 60 mm doublets. Because of the uncoated glass plate in the pump beam path, the incident pump power onto the crystal was 83% of the total diode power.

The cavity was a three-mirror V-shaped resonator: the back mirror was a plane dichroic mirror—high reflection (HR) coated over 1020–1200 nm on the rear face, and AR coated for pump wavelength on both faces. The folding mirror was a concave meniscus (radius of curvature $R = 200$ mm, HR coated over 1020–1200 nm, and also AR coated for pump wavelength on both faces in order to avoid detrimental feedback into the diode). The third mirror was a plane output coupler, whose transmission coefficient was chosen in order to maximize the output power of each crystal under test.

The path lengths between mirrors were chosen so that the laser operates in the single transverse (TEM_{00}) mode. The crystals were wrapped with indium foil and clamped in a copper block. The latter was maintained at 15 °C by a flow of circulating water. The transverse section of the crystals under investigation was between 3 and 5 mm square, which is one order of magnitude larger than the pumped area.

3. Thermal lensing in Yb:GdCOB

Yb:GdCOB is a broadband crystal which is particularly attractive for high power tunable and femtosecond lasers [4]. We will take this crystal as an example to discuss the tendencies that were also observed with the other materials treated in the next sections.

The crystal used in these experiments was 2.9 mm long, 15 at.% doped, AR coated on both faces, and cut along the Y crystallophysic axis. A pump power of 10.5 W at 976 nm was incident onto the
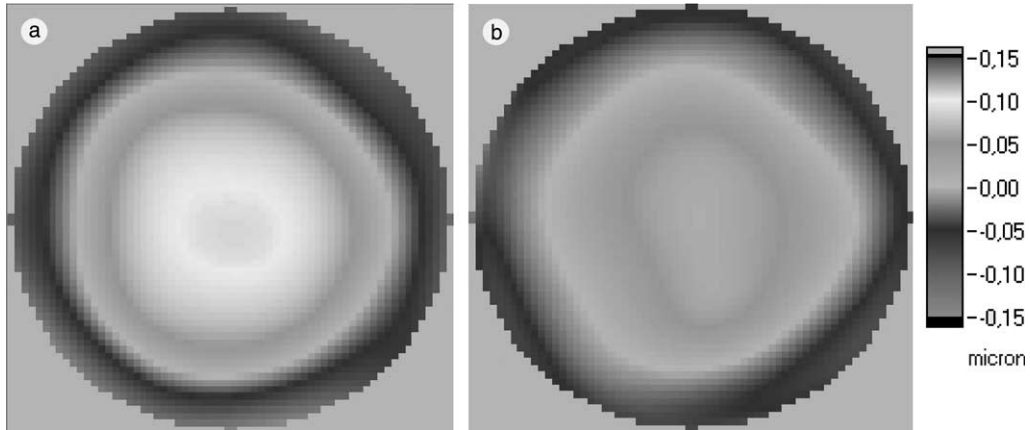
Fig. 2. Referenced wavefronts obtained with Yb:GdCOB (pupil diameter: 2.3 mm) at maximum diode power: (a) without laser action (peak-to-valley: 0.272 μm); (b) with laser action (peak-to-valley : 0.144 μm).

crystal. The recorded referenced wavefronts are shown in Fig. 2. We observed that the phase distortion only consisted of defocusing, all aberrations being negligible, as shown by the histogram of Zernike polynomials (up to fifth order) displayed in Fig. 3. In particular, the third order spherical aberration coefficient at the edge of the pupil, and the third order astigmatism, were both less than 0.01 microns. The absence of aberrations means that the index profile seen by the cavity beam is perfectly parabolic, and that therefore the thermal lens can be readily compensated.

The laser output power and the thermal lens dioptric power in m^{-1} are given in Fig. 4. The
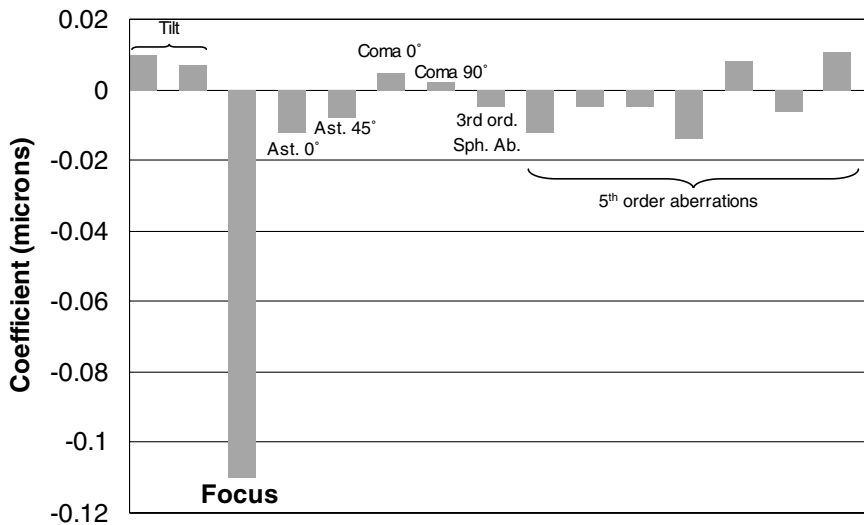
Ast. = astigmatism ;
3rd ord. Sph. Ab. = 3rd order spherical aberration.

Fig. 3. Zernike coefficients of the wavefront obtained with Yb:GdCOB without laser action. The diameter of the pupil is 2.3 mm. The coefficients are in microns and yield the amplitude of the aberration at the edge of the pupil.
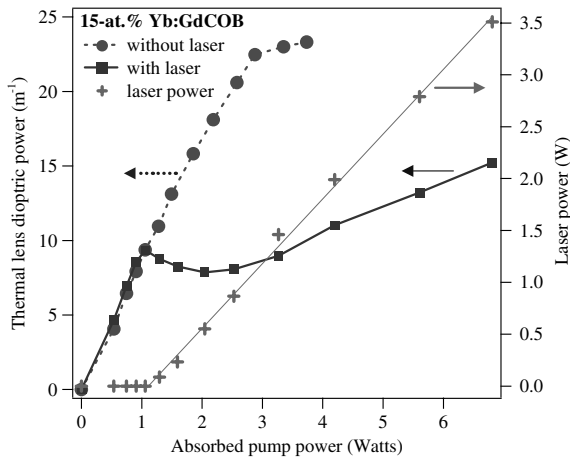
Fig. 4. Thermal lens dioptric power and laser power versus absorbed pump power in Yb:GdCOB.

crystal absorbed 6.8 W (when lasing) and 3.5 W of laser power were obtained. One can notice that the absorbed power is smaller under nonlasing conditions because of the strong saturation of absorption (which is lower when lasing because of the refilling of the $^2F_{7/2}$ manifold).

For a given absorbed pump power, the thermal lens is weaker (its focal length is longer) under lasing conditions. This puts clearly in evidence that extra heat-generating processes, other than quantum defect, contribute to a quenching of the excited state population. When lasing, these processes are shunted by laser extraction, resulting in a weaker thermal load. It's important to point out that nonradiative effects are commonly totally neglected in Yb-doped materials [11] since there are no additional energy levels (as in other trivalent rare-earth doped materials). The observed difference between thermal lensing with and without laser extraction can then be attributed to nonradiative sites ("dead sites") and concentration quenching [11]. The presence of nonradiative transfers may be connected to impurities or structural defects of the lattice: a complete investigation of these effects would thus require a systematic study of identical crystals grown under different conditions to find the physical origin of these phenomena.

Furthermore, one can notice that the dioptric power without laser action does not scale linearly

with the absorbed pump power but experiences a roll off. We propose that it is related to absorption saturation, together with the divergence of the pump inside the crystal.

We give in the following sections some examples of measurements carried out with other crystals.

4. Thermal lensing in Yb:YAG

We used a 8 at.% doped Yb:YAG crystal, 1.95 mm long, AR coated on both faces, grown at the CEA-LETI (Grenoble, France). The pump power incident onto the crystal was here 10.1 W, at 968 nm. 5.65 W were absorbed under lasing conditions and 2.68 W of laser power were then obtained. All the features pointed out in Yb:GdCOB are identical here (Fig. 5). We noticed the absence of thermal aberrations, and a significant difference between the thermal lens dioptric power under lasing and nonlasing conditions: the focal lengths were 12 and 5.2 cm, respectively, at maximum diode power. The interpretation may be the same that for GdCOB. However, as for GdCOB, complementary investigations are necessary to find out what mechanisms are responsible for nonradiative effects. Since only one crystal has been investigated so far, these results may not be interpreted by saying that such effects always arise in Yb:YAG, but that they cannot be a priori considered as
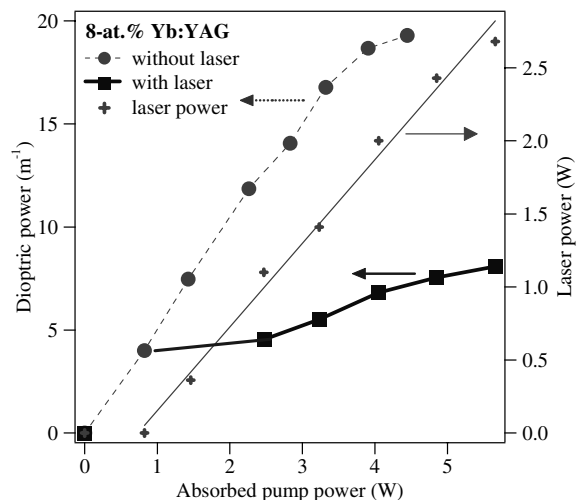

Fig. 5. Thermal lensing and laser efficiency of Yb:YAG.

inexistent in a sample whose radiative properties are not known.

5. Thermal lensing in Yb:KGW

We used a 5 at.% Yb:KGW crystal, from Eksma Inc., cut along the *c* axis, 3 mm long, AR coated on both faces. The incident power was 14.8 W, the crystal absorbed 6.8 W, and here 1.23 W of laser power were obtained. For this experiment the absorption was not optimized since the pump was at 979 nm whereas the absorption peak is at 981 nm. Results are given in Fig. 6. Thermal lensing is much weaker than for other crystals, for comparable absorbed powers. It can be seen that here, the thermal lens dioptric power is higher under lasing action. This can be attributed to the addition of two factors: (1) the radiative quantum efficiency approaches unity and (2) the mean fluorescence wavelength (993 nm) is much lower than the laser wavelength (1030 nm). That means that a stimulated photon generates more heat than a spontaneous photon.

6. Thermal lensing in Yb:YSO: dependence of thermal lensing with laser wavelength

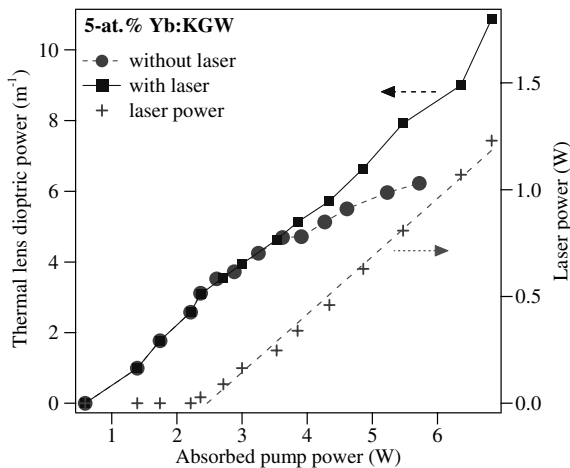The study of Yb:KGW makes clear that the lasing wavelength has a critical importance on thermal lensing. In broadly tunable materials, one can expect a dependence of the thermal load with the emitted wavelength since the quantum defect, when the pump wavelength is fixed, depends on the lasing level.

To clearly put in evidence this effect, we used a Yb:Y_2SiO_5 (Yb:YSO) [6] crystal: it is well suited to make this experiment since its emission spectrum exhibits two bumps of comparable magnitude at 1042 and 1058 nm. We used here a 1.95 mm long, 5 at.% doped crystal, cut for propagation along the *X* axis (YSO is biaxial). The incident power was 11.8 W at 977 nm, and the crystal absorbed 6.8 W under lasing action.

The tuning of the laser wavelength was achieved by introducing a dispersive SF6 prism in the collimated arm of the three-mirror cavity. Results are shown in Fig. 7. The output power was 2.1 W at both wavelengths, with similar slope efficiencies and thresholds. Strong thermal lensing is observed (the thermal lens focal length equals 3.2 cm under lasing action, at 1058 nm) and one can see that thermal effects are indeed weaker when lasing at 1042 nm (3.8 cm), corresponding to a smaller quantum defect, as expected. This experiment illustrates the fact that when designing a high power Yb laser, one must carefully take care of the lasing wavelength (which may vary over a large interval depending on
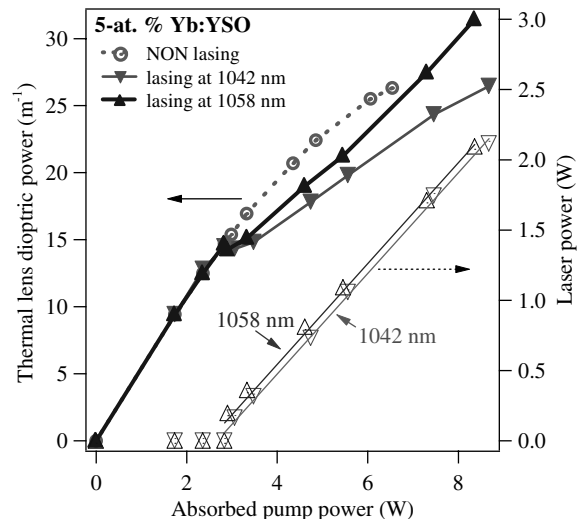
Fig. 6. Thermal lensing in Yb:KGW.

Fig. 7. Thermal lensing in Yb:YSO (Yb:Y_2SiO_5) at two wavelengths (1042 and 1058 nm) for identical absorbed and laser power.

the output coupler transmission): if it is too low, reabsorption losses make the laser working less efficiently; if it is too high, thermal lensing is stronger.

7. Reduction of thermal effects with a composite YCOB/Yb:YCOB crystal

An efficient solution to reduce thermal effects in end-pumped lasers is the use of composite materials [12]: they are made of doped crystals diffusion-bonded on undoped crystals used to dissipate heat in the direction of pumping. We tested such a composite, realized (cut, polished and bonded) at the Laboratoire de Chimie Appliquée de l'Etat Solide, which consisted of an Yb-doped YCOB crystal diffusion-bonded on an undoped YCOB crystal [13]. YCOB is an oxoborate crystal whose properties are similar to these of GdCOB [5]. We compared it to a homogeneous Yb-doped YCOB crystal as far as performance and thermal lensing are concerned. Both crystals were cut from the same boule, so that they had identical optical quality and doping concentration (15 at.%).

The crystals were cut so that the propagation vector k is along the crystallophysic X axis. The single rod (homogeneously doped) crystal was 2.5 mm long; the composite crystal was made of a 1.9 mm long doped part bonded on a 1.45 mm undoped cap. Both of them were AR coated. Fig. 8
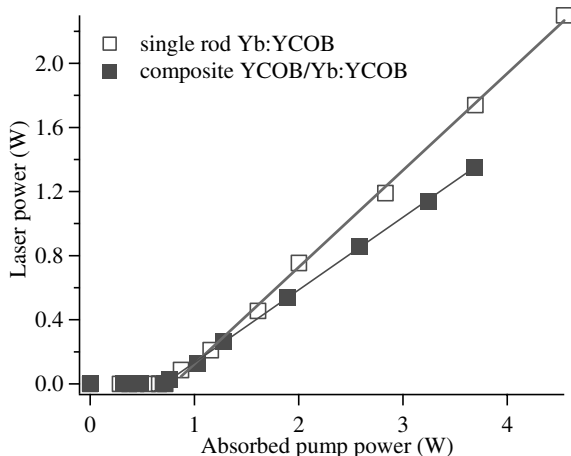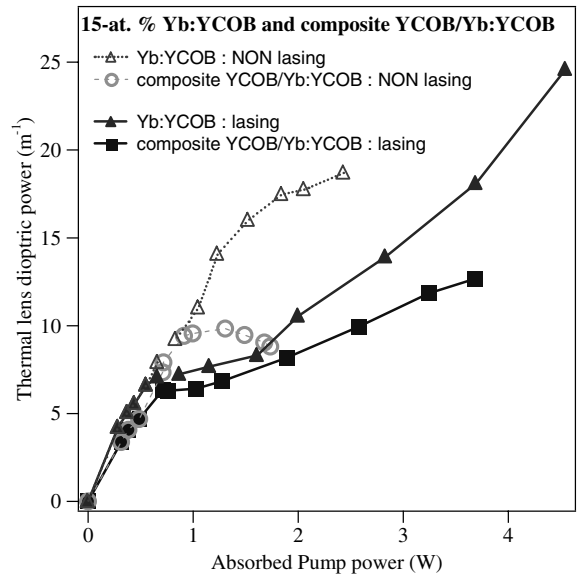

Fig. 9. Thermal lensing in single rod (dashed line) and composite (solid line) Yb:YCOB crystals.

shows the compared laser performance of the two crystals: the absorbed power is different because the two crystals did not have the same lengths. The slope efficiency appears to be also slightly lower for the composite crystal, what may be attributed to losses at the interface.

Thermal lensing measurements results are shown in Fig. 9: as expected, the thermal lens dioptric power was approximately two times weaker under nonlasing conditions in the composite YCOB crystal than in the homogeneous Yb:YCOB crystal. Under lasing action the same tendency is observed.

8. Thumb rule for power scaling

Table 1 summarizes the results described above. For comparison, the thermal lens focal length (in mm) is given under lasing action at the same absorbed pump power (5 W) for every crystal. However, when scaling these lasers to higher output powers, while keeping the same pumping scheme (that is under fiber-coupled end pumping), it is very useful to predict the value of the thermal lens under laser action. The good parameter to use

Fig. 8. Laser performance of Yb:YCOB (single rod crystal) and composite undoped YCOB/Yb:YCOB crystal.

Table 1
Overview of crystal properties and experimental results

Crystal	Yb:GdCOB	Yb:YCOB		Yb:YSO	Yb:YAG	Yb:YSO
		Single rod	Composite			
Crystal length (mm)	2.9	2.5	1.9 (+1.45 mm undoped)	1.95	1.95	3
Orientation (k = wavevector)	$k\|Y$	$k\|X$	$k\|X$	$k\|X$	Isotropic	$k\|c$
Pump wavelength (nm)	976	976	976	977	968	979
Doping level (%) (corresponding atomic concentration in ions/cm^3)	15% (6.6×10^{20})	15% (6.7×10^{20})	15% (6.7×10^{20})	5% (9.2×10^{20})	8% (11×10^{20})	5% (2.2×10^{20})
Thermal lens focal length for 5 W of absorbed pump power under *lasing conditions* (mm)	81	36	60	54 @ 1042 50 @ 1058	130	143
"Thermal loading slope" η_{SL}, under *lasing conditions* (see text) $\times 10^{-8}$ m^{-1}/(W m^{-2})	5.3	17	7.6	7 @ 1042 nm 10.1 @ 1058 nm	3.6	5.3

is then the slope of the straight line fitting the thermal lens dioptric power versus absorbed pump power, under lasing action. This slope gives an indication of how the thermal lens increases when the pump power is increased. But in end-pumped lasers, the thermal lens dioptric power scales inversely with the pumped area [14], which then must be larger in the crystal at higher pumping powers in order to avoid thermal fracture. The parameter of interest for power scaling is therefore the slope per unit surface, what is called here the "thermal loading slope" η_{SL} expressed in m^{-1}/ (W m^{-2}): this value appears in Table 1.

From η_{SL} and from the value of the focal length at 5 W of absorbed power $f_{th}(5\ W)$, one can then deduce for each crystal the focal length f_{th} at an arbitrary absorbed power P_{abs}:

$$\frac{1}{f_{th}} = \frac{1}{f_{th}(5\ \mathrm{W})} + \eta_{SL}\left(\frac{P_{abs}}{S} - 1.610^8\right)$$

where S is the surface of the pumped area (in m^2).

The most favorable materials (with lower η_{SL}) turn out to be YAG, KGW and GdCOB. Since the dioptric power is not proportional to the absorbed power at all powers but is in fact described approximately by two distinct slopes (separated by the laser threshold), this makes possible the situation encountered here with GdCOB and KGW:

for 5 W of absorbed power the thermal lens focal length is nearly twice as long in KGW, whereas the thermal loading slopes are the same.

9. Conclusions

A method for measuring thermal lensing in end-diode-pumped crystals is presented and has been used to investigate thermal effects in Yb-doped GdCOB, YCOB, YAG, KGW, YSO, and composite YCOB. We demonstrated, for the first time to our knowledge in Yb-doped materials, that thermal lensing was stronger under nonlasing conditions than under lasing conditions, for a given absorbed power. It is a proof that significant nonradiative transfers occur in Yb-doped materials, contrary to what is generally admitted. We have shown that thermal lensing was reduced by a factor of two by using a composite crystal (made of a doped Yb:YCOB crystal diffusion-bonded on an undoped YCOB cap). By making thermal lensing measurements in Yb:YSO, we showed that the thermal load was depending on the emission wavelength, as expected from quantum defect considerations. The measurements performed here under lasing action can be used for the design of high power fiber-coupled diode-pumped lasers based on these crystals.

References

[1] W.A. Clarkson, J. Phys. D: Appl. Phys. 34 (2001) 2381.

[2] L.D. DeLoach, S.A. Payne, L.L. Chase, L.K. Smith, W.L. Kway, W. Krupke, IEEE J. Quant. Electron. 29 (1993) 1179.

[3] F. Mougel, K. Dardenne, G. Aka, A. Kahn-Harari, D. Vivien, J. Opt. Soc. Am. 16 (1999) 164.

[4] S. Chénais, F. Druon, F. Balembois, G. Lucas-Leclin, P. Georges, A. Brun, M. Zavelani-Rossi, F. Augé, J.P. Chambaret, G. Aka, D. Vivien, Appl. Phys. B 72 (2001) 389.

[5] N. Zhang, X. Meng, P. Wang, L. Zhu, X. Liu, R. Cheng, J. Dawes, P. Dekker, S. Zhang, L. Sun, Appl. Phys. B 68 (1999) 1147.

[6] R. Gaumé, P.-H. Haumesser, B. Viana, G. Aka, D. Vivien, E. Scheer, P. Bourdon, B. Ferrand, M. Jacquet, N. Lenain, in: OSA Trends in Optics and Photonics (TOPS), Vol. 34, Advanced Solid State Lasers, OSA Technical digest, Postconference edition (optical Society of America, Washington DC, 2000), p. 469.

[7] P. Lacovara, H.K. Choi, C.A. Wang, R.L. Aggarwal, T.Y. Fan, Opt. Lett. 16 (14) (1991) 1089.

[8] A.A. Lagatsky, N.V. Kuleshov, V.P. Mikhailov, Opt. Comm. 165 (1999) 71.

[9] D.J. Armstrong, J. Mansell, D. Neal, Laser Focus World 34 (1998) 129.

[10] M. Born, E. Wolf, Principles of Optics, Pergamon Press, London, 1965.

[11] T.Y. Fan, IEEE J. Quant. Electron. 29 (6) (1993) 1457.

[12] M. Tsunekane, N. Taguchi, H. Inaba, Appl. Opt. 37 (15) (1998) 3290.

[13] R. Gaumé, B. Viana, D. Vivien, G.P. Aka, in: OSA Advanced Solid State Lasers 2002, Technical digest, Conference edition (optical Society of America, Washington DC, 2002), paper WB2.

[14] M.E. Innocenzi, H.T. Yura, C.L. Fincher, R.A. Fields, Appl. Phys. Lett. 56 (19) (1990) 1831.